Magnetic compound refractive lens for focusing and polarizing cold neutron beams

K. C. Littrell, S. G. E. te Velthuis, and G. P. Felcher
Argonne National Laboratory, Argonne, Illinois 60439

S. Park, B. J. Kirby, and M. R. Fitzsimmons
Los Alamos National Laboratory, Los Alamos, New Mexico 87545

(Received 13 November 2006; accepted 25 January 2007; published online 9 March 2007)

Biconcave cylindrical lenses are used to focus beams of x rays or neutrons using the refractive properties of matter. In the case of neutrons, the refractive properties of magnetic induction can similarly focus and simultaneously polarize the neutron beam without the concomitant attenuation of matter. This concept of a magnetic refractive lens was tested using a compound lens consisting of 99 pairs of cylindrical permanent magnets. The assembly successfully focused the intensity of a white beam of cold neutrons of one spin state at the detector, while defocusing the other. This experiment confirmed that a lens of this nature may boost the intensity locally by almost an order of magnitude and create a polarized beam. An estimate of the performance of a more practically dimensioned device suitable for incorporation in reflectometers and slit-geometry small angle scattering instruments is given. © *2007 American Institute of Physics.* [DOI: 10.1063/1.2709844]

INTRODUCTION

Most neutron scattering experiments are intensity limited and many are also resolution limited. With instruments based on slit or pinhole collimation, intensity and resolution are intimately linked by geometry. However, this linkage can be broken through the use of optics that focuses the intensity onto a small area. In the case of an instrument that requires a polarized beam, magnetic focusing can be used with the advantage that it modifies the beam without placing additional scattering or absorbing material in it. Great progress has been made recently in the development of magnetic focusing for a pinhole geometry by means of Halbach-type sextupole lenses.[1–3] This geometry is best suited for small angle scattering instruments. Here instead, we discuss a compound magnetic refractive lens more appropriate to the slit geometry that is used in reflectometers. The term compound refers to a sequence of individual lenses that together can be considered to constitute a single lens. The geometry of the beam is a slit offering fine collimation along its width, but providing a broad beam along its height. The purpose of this device is to focus the beam along its height, where a changed divergence will not be of importance.

In 1996 Snigivev *et al.*[4] proposed and demonstrated that x-ray refractive focusing could be accomplished with a linear array of many elementary lenses made of low-Z material. Lens of low-Z materials are desirable, because their absorption is relatively weak compared to high-Z materials. Following the first successful demonstration, many publications describing further developments have appeared.[5–7] Similar lenses have been developed for the focusing of cold neutron beams.[8,9] The basic idea of the refractive lens is the following. In general, the refractive index is

$$n^2 = 1 - (V/E), \tag{1}$$

which is given in terms of the potential energy V and the kinetic energy E of the radiation. For neutrons in matter $V \cong h^2 Nb/2\pi m$ and $E = h^2/2m\lambda^2$, where h is Planck's constant, N is the number density of atoms in the material, b is the average bound coherent scattering length of these atoms, m is the neutron's mass, and λ is its wavelength. This leads to an index of refraction as a function of wavelength λ given by

$$n \cong 1 - \frac{\lambda^2 Nb}{2\pi}. \tag{2}$$

Since $n < 1$ for materials with $b > 0$, a cylindrical void in the material, with the axis perpendicular to the neutron path, will constitute a focusing refractive lens. The focal length of a lens, within the thin lens approximation, is given by[10]

$$\frac{1}{f_1} \cong \frac{2(n-1)}{r}, \tag{3}$$

where r is the radius of curvature of the cylindrical lens.

A disadvantage of lenses composed of matter is that they attenuate the neutron beam through absorption and scattering. At present, the most efficient material lenses for neutrons[9] are composed of MgF_2 because of its transparency. Its scattering amplitude density $Nb = 5.06 \times 10^{10}$ cm^{-2}, a value which is typical for material lenses. The resulting index of refraction for a neutron wavelength of 4 Å—a characteristic wavelength for neutrons moderated in liquid hydrogen—is only weakly different from 1, in fact, $1 - n = 1.3 \times 10^{-5}$. Generally, material lenses are spin insensitive—both spin states of the neutron are focused (or defocused) in the same way.

For neutrons, a change in the refractive index comparable in magnitude to that for matter can also be achieved by

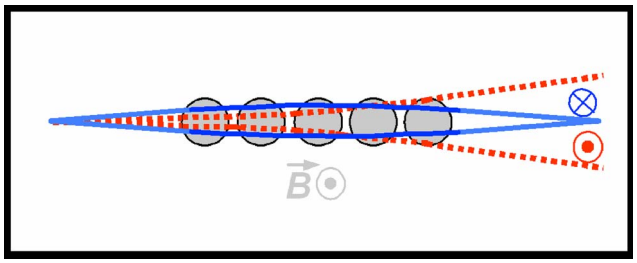

FIG. 1. (Color online) Schematic drawing of working of the compound magnetic refractive lens. The circular areas represent regions with a magnetic induction B directed out of the plane of this sketch. As the neutron beam passed through, the beam is refracted at the edges of the circular regions. This refraction process is different for neutron spins that are parallel (spin up) and antiparallel (spin down) to the magnetic induction B, resulting in the focusing of the neutrons of one spin state (blue, solid) and the defocusing of the other (red, dotted).

a magnetic field. In this case the potential energy V in Eq. (1) is given by the magnetic potential energy $V=-\boldsymbol{\mu}\cdot\mathbf{B}$, where μ is the neutron's magnetic moment, and $\mathbf{B}$ is the magnetic induction. In this expression the neutron moment is considered classically. However, the relations that will be derived are correct even if $\boldsymbol{\mu}$ is considered a quantum mechanical quantity.

Therefore, a single round region of magnetic field, as might be created between two cylindrical magnets of radius r placed alongside the beam, constitutes a magnetic lens[11] and likewise focuses the neutron beam intensity. Using Eqs. (1) and (3) the focal length of the magnetic lens is calculated to be

$$\frac{1}{f_1} \cong \pm \frac{2|\mu|Bm\lambda^2}{rh^2}. \tag{4}$$

The signs in Eq. (4) indicate that the magnetic lens is birefringent. Neutrons with a moment parallel (but spin opposite) to $\mathbf{B}$ are focused while those with a moment opposite (but spin parallel) to $\mathbf{B}$ are defocused. With a magnetic field $B=2.25$ T, a magnetic lens has the same focusing power as a MgF_2 lens of the same geometry.

A sequence of N cylindrical voids or magnetic field regions constitutes a compound lens and correspondingly shortens the focal length by

$$f_N = f_1/N, \tag{5}$$

if the actual length of the lens is not taken into account, as in the thin lens approximation. A sketch of the principle of the compound magnetic refractive lens (CMRL) is given in Fig. 1. Although the refractive index for neutrons is quite small, the effect of magnetic focusing is not negligible. For instance, for $r=1$ cm, $B=1$ T, and $N=100$ elements, a neutron beam with a wavelength of 8 Å has a focal length, according to Eqs. (4) and (5), of 2.1 m.

The next section describes our tests of a compact CMRL. In the following section the characteristics of this lens are compared with another type of magnetic lens, the Halbach-type sextupole. The final section discusses how a CMRL may become a device conveniently shaping the beam in front of reflectometers at steady state and pulsed neutron sources.

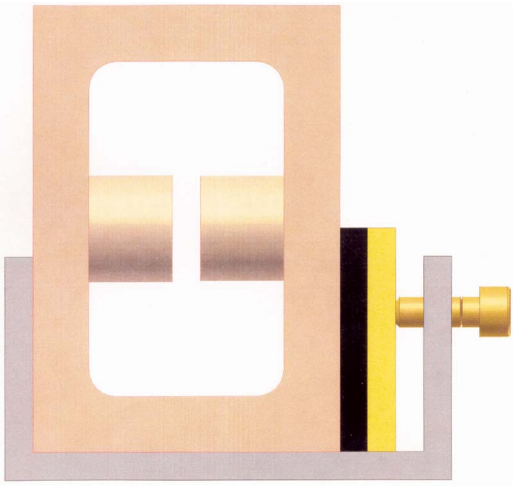

FIG. 2. (Color online) Sketch of one magnetic assembly of the CMRL tested on ASTERIX. The assembly consists of a rectangular steel frame (outer dimension: 5.08×3.5 cm^2), providing the return path of the magnetic flux of two NdFeB cylindrical magnets (1.27 cm diameter). The magnetic field in the open space is mostly confined to the 3 mm gap between the two magnets crossed by the neutron beam.

EXPERIMENT

The lens consisted of an ensemble of 99 H-type permanent magnet assemblies (Fig. 2). In each assembly, the magnetic field was provided by two cylindrical permanent magnets made of nickel plated sintered NdFeB. Each magnet had a 1.27 cm diameter, 0.95 cm thickness, and a remanence of 1.37 T.[12] They were placed inside a frame of AISI 10-18 hot rolled steel to enable magnetic flux closure. The magnetic field in the 3 mm gap was found to be 1.01 T±0.03 for all magnets. The magnets were aligned in an aluminum rail guide and set apart with a 3 mm gap using polyethylene spacers. In this geometry, the magnetic field drops to near zero in the gap between adjacent magnets, maximizing the relative refractive index. The lens had a total length of 157.5 cm. Its overall design was dictated by the need of creating a device as compact as possible and yet strong enough to obtain significant focusing of the neutron beam.

The lens was tested (Fig. 3) on the polarized neutron reflectometer "ASTERIX" (Ref. 13) at the Los Alamos Neutron Scattering Center (LANSCE) of Los Alamos National Laboratory, which is a pulsed spallation neutron source. ASTERIX has a polarized neutron beam, with a polarization efficiency of 93.5% that is fairly constant across the total measurable wavelength range of 4–13 Å. A radio-frequency-gradient-field spin flipper[13,14] installed after the polarizer allows the magnetic moment of the neutrons to be parallel or flipped opposite to the guide field that exists along the rest of the flight path.

In the experimental arrangement (Fig. 4), the incoming beam was defined horizontally by two slits, each 0.4 mm wide, and located at 130 and 43 cm from the entrance of the lens. These slits limited the horizontal divergence, which was necessary to ensure the beam stayed within the 3 mm gap between the pairs of magnets. Vertically the beam was defined by a slit 2 mm high and aligned with the center of the active area of the lens and at a distance of 24 cm from the

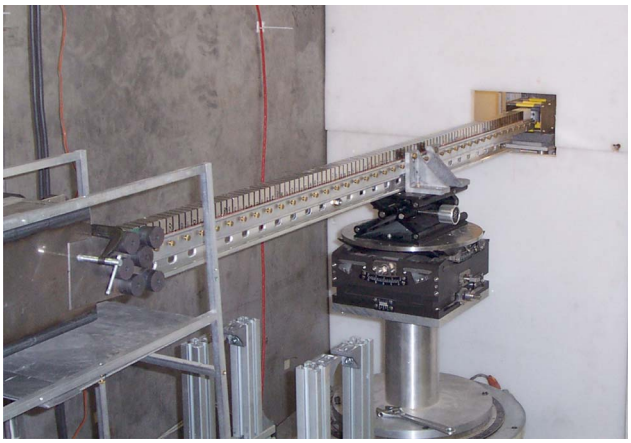

FIG. 3. (Color online) Picture of the compound refractive lens during the experiments on ASTERIX. In this image the outside of the 99 magnetic frames, mounted on the aluminum rail guide and placed on the sample goniometer, can be seen at the center of the image. The total length of the lens is 157.5 cm. The beam originates from the source in the top right, and passes through the center of the lens towards the bottom left, where 146 cm later it reaches the detector.

entrance of the lens. The vertical divergence before this slit, as dictated by the characteristics of the upstream neutron guides, is 0.1 deg/Å. The end of the lens was at a distance of 146 cm from the detector, leaving ample space for the polarization analyzer that was inserted for some of the measurements in order to check if the polarization of the beam was maintained after passing through the lens. Although the orientation of the guide fields of the instrument, and thereby incident polarization axis, was perpendicular to that of the field between the magnets of the lens, an adiabatic 90° rotation of the polarization was achieved by adding a small guide field before the lens. As a result the polarization was along the direction of the field in the lens as the neutron beam enters the lens. As the focusing action of the lens is along the vertical direction, the linear position-sensitive detector was oriented with its position-sensitive direction vertical in most of the experiments.

Figures 5(a) and 5(b) show the intensities as a function of wavelength and vertical detector position measured with the lens installed when the neutron spin is antiparallel (spin down) and parallel (spin up) to the field between the magnets, respectively. The background intensity has been subtracted and the intensities have been normalized to the incident spectrum. The large fluctuations of the intensity at long wavelengths are explained by lower intensities and hence poor counting statistics due to the fact that the incident spectrum decays with λ^4. The large statistical error around 9 Å, coincident with the beginning of the second time frame, is due to the fact that a large background, which is the result of a flash of composite radiation created by the proton pulse hitting the target, has been subtracted.[13]

Figure 5(a) clearly shows the focusing effect of the lens as the height of the beam at the detector decreases signifi-

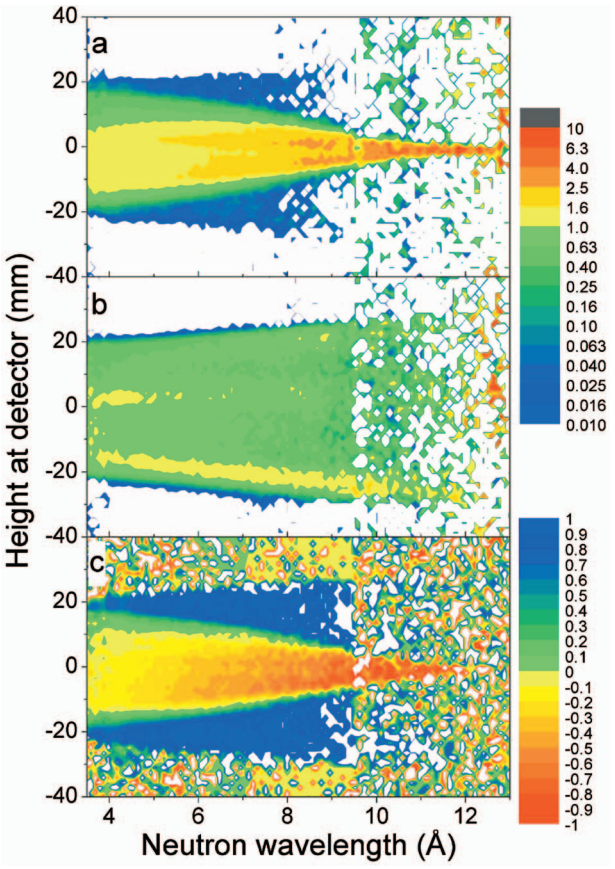

FIG. 5. (Color) (a) Intensity as a function of vertical detector position for neutrons with spin state antiparallel (spin down) to the field. The intensities have been normalized to the wavelength spectrum. The initial height of the beam was 39 mm for all wavelengths. (b) Intensities for neutrons with spin state parallel (spin up) to the field. (c) The polarization of the beam calculated using the intensities of Figs. 5(a) and 5(b).

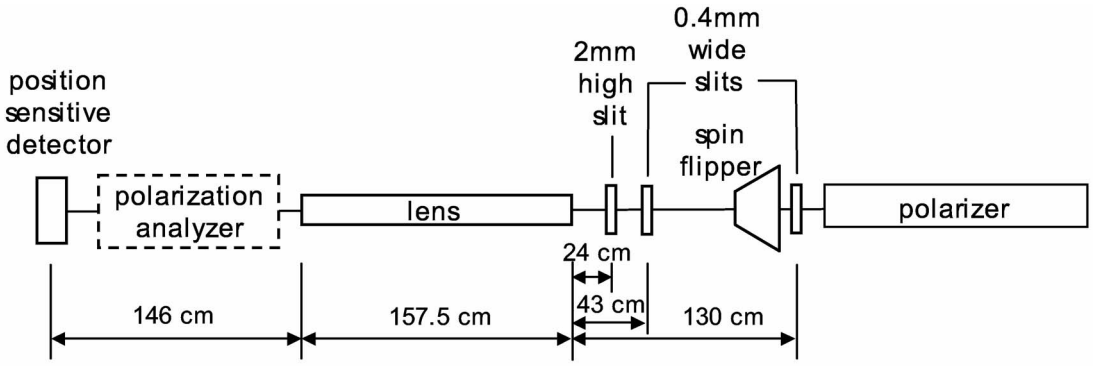

FIG. 4. Schematic diagram of the compound refractive lens on the ASTERIX instrument.

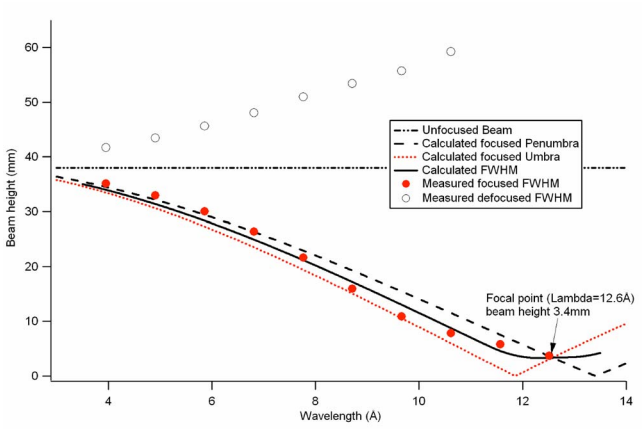

FIG. 6. Comparison of the experimental and calculated height of the beam at the detector. The calculation is smeared by a 1 Å running average in wavelength to match the averaging of the measured values.

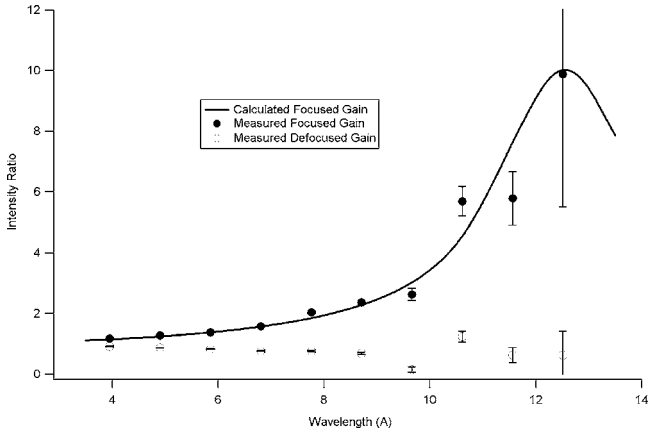

FIG. 7. Comparison of the experimental and calculated enhancement of the intensity. The calculation is smeared by a 1 Å running average in wavelength to match the averaging of the measured values.

cantly for increasing wavelength, paired with an increase in the peak intensity. Consistently, Fig. 5(b) shows the defocusing effect of the lens for neutrons with the other spin state, as the beam gets higher with increasing wavelength. The defocusing effect is less dramatic because the neutrons are not further defocused once they diverge above and below the regions of strong magnetic field created between the magnets. There are some variations in intensity as a function of height, but these were also present in measurements performed without the lens, and are therefore a characteristic of the incident beam.

Figure 5(c) presents the polarization, defined as $(I^{\mathrm{up}}-I^{\mathrm{down}})/(I^{\mathrm{up}}+I^{\mathrm{down}})$, calculated for each detector position and wavelength. The result is impressive as the polarization at the long wavelengths is close to −1. In practice, if a lens has focusing properties similar to that in this setup there is no need to polarize the beam in advance. As a matter of fact, it has long been known that magnetic gradients constitute the cleanest way to polarize a neutron beam. This property is also vividly demonstrated by a particular feature in our experiment. As mentioned, the beam on ASTERIX was polarized *only* by 93.5%. As can be seen in Fig. 5(a), at the outer edge of the focused beam there is a weak outward flare of intensity. This flare has the same shape as the defocused beam shown in Fig. 5(b). By placing a polarization analyzer after the lens, we were able to verify that this flare was indeed due to the 6.5% of the neutrons in the beam that had the opposite polarization.

The experimental data are compared to calculations based on the system's optics; details of which are presented in the Appendix. The comparison between experiment and calculation is crucial, because if satisfactory, it indicates how much the design of a practical lens can be advanced without recurring to a cumbersome sequence of experimental tests. Applying Eqs. (5) and (A3)–(A5) gives 12.6 Å as the wavelength at which the 2 mm high "object" slit is maximally focused at the detector. The values of the intermediate calculated quantities that give the optical properties of the lens are the thin lens focal length $f_N=48$ cm, the effective focal length $f=101$ cm, and the principal plane distance $d=138$ cm. Figure 6 shows the height of the beam originating from the 2 mm high object derived from the positions of the extreme edges of the beam as calculated using Eq. (A1). The focal point is where the trajectory of the umbra and penumbra points crosses, and occurs at $\lambda=12.6$ Å. Figure 6 shows that the calculated values closely match the corresponding experimental values. The expected gain in intensity at the detector can be estimated by determining the reduction in the height of the beam due to the focusing action of the lens. Without the lens, the 2 mm high slit illuminates the detector over a total height of 39 mm. With the lens, the minimum height occurring at $\lambda=12.6$ Å is 3.4 mm. This tenfold reduction means that the intensity should increase by a factor of 10. Figure 7 presents the gain in intensity as calculated and as obtained experimentally from the ratio of intensities of the detector pixel at the center of the beam measured with and without the lens. Again there is substantial agreement between the expected and measured values. The agreement between experimental and calculated values confirms that two constraints of the calculation are basically correct. The first hypothesis, that the neutron spin follows adiabatically the magnetic field, is satisfied by the fact that the Larmor precession frequency of the neutron spin is higher, by two orders of magnitude, than the frequency of modulation of the magnetic field. The second hypothesis is that there is only one direction along which the magnetic fields are aligned throughout the magnetic lens. This second hypothesis is fairly well, but not completely satisfied; it is worthwhile to discuss the extent of the perturbation.

Ideally the lens would only have an effect on the beam in the vertical direction, leaving the well collimated horizontal beam unchanged. To check this, measurements were also performed with the detector rotated by 90° so that the direction in which the detector is position sensitive is horizontal. Since this measurement was limited to a relatively short time, statistics prevented the full display of the intensity distribution as a function of wavelength. Instead, Fig. 8 shows the position dependent intensity for the two spin states integrated over the complete wavelength spectrum. From this figure it is clear that the spin down neutrons, that were focused in the vertical direction, are now defocused in the horizontal plane. However, these opposing effects are not intrin-

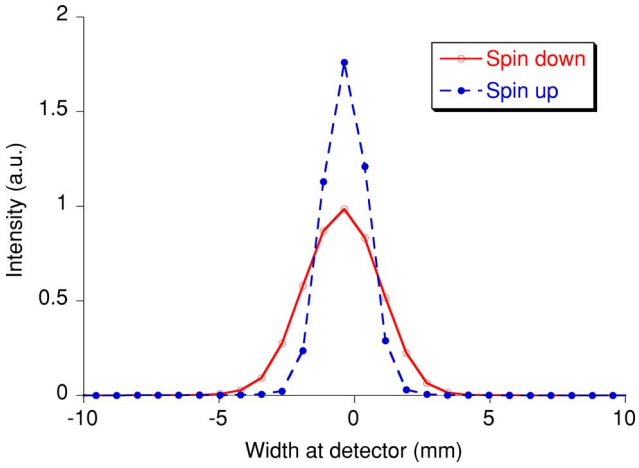

FIG. 8. (Color online) Horizontal beam profile for the two spin states, summed over all wavelengths.

sic to this lens. It has been demonstrated[11] that it is simply due to the fact that the magnetic field lines across the gap between the two magnets are not straight but tend to bulge, creating also a magnetic gradient in the horizontal direction that again acts as a refractive lens. It has been shown[11] that this inconvenient feature can be suppressed by reshaping the front of the magnets (or pole pieces). In fact, by appropriately tapering the pole faces, the neutron beam can be focused in both directions for the spin down polarization.

COMPARISON WITH MAGNETIC SEXTUPOLE LENSES

The only other magnetic lens hitherto developed for cold neutrons is the sextupole lens, created to focus a pinpoint source onto the detector. In the sextupole lens the magnetic field gradient is strictly perpendicular to the beam direction, and the cross section of the magnetic fields is uniform along the lens' axis. For the sextupole it can be derived (see the Appendix) that the focal length is given by

$$\frac{1}{f_L} \cong \frac{2|\mu|B_{\max} m\lambda^2 L}{r_a^2 h^2}, \tag{6}$$

where r_a is aperture radius over which there is a gradient field, and L is the total length of the sextupole lens. Equation (6) is equal to Eq. (5) with the substitution $L/r_a^2 = N/r$. For the CMRL $N = L/(2r+g)$, where g is the gap between subsequent magnetic cylinders. It follows then that, if the field at the rim of the aperture of the sextupole and the magnetic field in the gap of the CMRL magnet are equal, the sextupole lens has approximately twice the focusing power per unit length of a CMRL with the same radius as for these circumstances.

The most modern sextupole lens is the Halbach arrangement that forms the heart of the JAEA JRR-3 focused small angle neutron scattering (SANS) instrument.[3] This lens has an aperture diameter of 25 mm and a length of 300 mm; the magnitude of the magnetic field at 10 mm from the center is 0.98 T. This very compact lens was demonstrated to focus ~9.75 Å neutrons in a symmetric configuration with object and image distances of 9.85 m. This mature design followed a first version of the Halbach design sextupole, where a magnetic field of 1 T was obtained only at a radius $r_a = 0.5$ cm, because the poles consisted of permanent magnets with a low saturation magnetization.

The role of the sextupole lenses in front of a small angle scattering instrument is quite exacting. The converging beam has to illuminate the sample and have its focal point at the detector. Any defocusing at the detector substantially reduces the gain in intensity provided by the device because it increases the low angle limit of the accessible momentum transfers. The situation for the CMRL is quite different. The CMRL is targeted for use in slit-geometry systems, for instance, in reflectometry. It is well known that in reflectometry the angular resolution along the slit is unimportant. Thus, the only requirement for the lens is that it brings a beam as intense as possible to illuminate the sample. The detector does not need to be a focal point of the optical system. The same is true of a new class of instruments designed to measure the scattering at grazing incidence, in particular, the scattering perpendicular to the reflection plane.[15] These instruments use spin-echo methods to determine the angle,[15,16] and thereby the lateral momentum transfer, of the grazing incidence scattering with a precision that is independent of the angular resolution of the incident or of the scattered beam. The CMRL is therefore also compatible with these new instruments if the focusing occurs in the same direction as the spin-echo analysis. Since the sole role of the CMRL is to maximize the intensity and the polarization over the lateral footprint of a sample, a few centimeters in size, the design constraints are considerably more relaxed than for the sextupole lenses, thereby making its construction relatively simple.

APPROACHING A PRACTICAL DEVICE

It is clear that the CMRL we tested can be improved on several accounts. Magnetic fields and magnetic field gradients can be increased by redesigning the permanent magnet assembly by choosing materials for the return-field yoke (and possibly pole pieces) that have the optimal magnetic properties and by optimizing the geometry of the assembly. For the single components of the CMRL we chose, out of convenience, a cylindrical geometry. However, this geometry is an approximation to the ideal parabolic section that is valid only in the paraxial limit, where neutrons are incident on the lens near its center on trajectories that are close to perpendicular to the lens surface. Recent x-ray lenses[17–19] have been designed substituting elements of circular profile with elements consisting of two parabolic segments facing each other. Additionally, the CMRL tested is too limited in size, the beam height too small, and the 3 mm gap too narrow to be directly incorporated in an instrument. The design of a practical CMRL requires a careful layout of the source and of the instrument to which the CMRL has to be integrated. Here an attempt is made to come to a design, more realistic in its dimensions, for which the performance is calculated.

As an illustration, we will consider the polarized-beam reflectometer viewing a pulsed neutron source with the char-

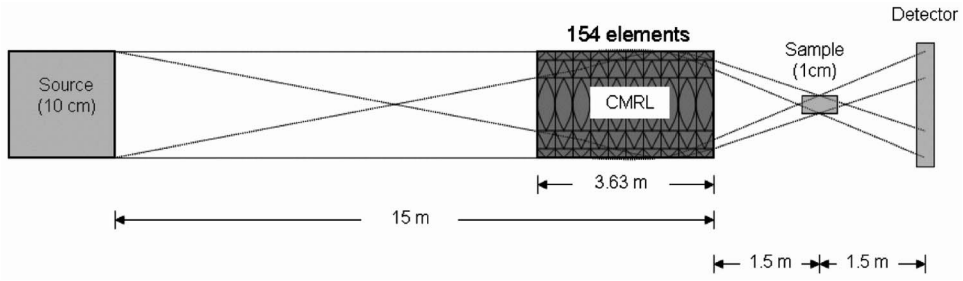

FIG. 9. The schematic of a more practically sized CMRL positioned within a neutron scattering instrument. The concept instrument has a 3.63 m long and 10 cm high CMRL consisting of 154 three-step Fresnel elements with a gap field of 1 T. The neutron spectrum is 3.66 Å wide, centered at 7 Å.

acteristics of the Spallation Neutron Source (SNS) in Oak Ridge[20]—with a pulse frequency of 60 Hz—shown in Fig. 9. Assuming the detector of the reflectometer is located at 18 m from the source gives a usable wavelength band of 3.66 Å which can be centered about any wavelength. We assume that the exit end of the lens is located at 1.5 m from the sample and 3 m from the detector, with the space before and after the sample being used for filters, flippers, spin-precession devices, or any other required beam conditioning components. For the purpose of calculating a gain factor, the moderator, which is the effective object, is chosen to be 10 cm high, the lens is taken to be the same height, and the sample is assumed to be 1 cm high. The gain factor is then the ratio of the intensity on the sample with the lens to the intensity on the sample without the lens. An ideal thin lens in this geometry would produce a peak gain of 10.

For a real device, it is reasonable to assume that with a proper design of the magnetic return-field circuit the gap between the pole pieces can be increased to 1 cm (or perhaps more) while retaining a maximum field in the gap of 1 T; this assumption is based on the fact that sextupole magnetic lenses with a maximum magnetic field of 1 T and a diameter of more than 2 cm have already been constructed using permanent magnets of the same type used in our experiment.[2] For the lens elements, we have chosen a biconvex, three-segment Fresnel-type segmented lens[21–23] with a parabolic profile. The dimension of such a lens element and the advantages of this design are shown in Fig. 10. As a comparison between the dotted and dashed curves indicates, the biconvex parabolic surface has the same paraxial radius of curvature—and thus the same focal length—as a circular lens with a length smaller by the square root of 2, increasing the active height of the lens. Furthermore, the focusing is uniform across the profile of the parabolic lens while it varies tremendously as the edge of the circular lens is approached. We assumed the biconvex profile for the inscribed circle purely for convenience; with the parabolic profile in a many-element lens, the number of elements and their individual thicknesses vary as a function of the parabola curvature for a lens of fixed total length and element thickness, but the focal length and overall performance of a perfectly manufactured lens do not. The advantage of the Fresnel design comes from the fact that the total length of the lens is reduced proportionally to the number of steps, producing a shorter lens for the same height and curvature and, hence, focal length.

With a source-to-detector distance of 18 m, a CMRL composed of straight parabolic lenses would be too long—longer than the instrument itself—if a center wavelength of 7 Å is chosen. On the other hand, a parabolic Fresnel lens with three steps (solid curve in Fig. 10) 3.63 m long (154 elements) will image the source at the sample with an average gain of 3.91 for the full wavelength range of 5.17–8.83 Å and over 4.4 between 6.17 and 7.79 Å. The calculated intensity gain as a function of wavelength is shown in Fig. 11. A three-step Fresnel lens is a good compromise: if more steps are used, the lens can be made shorter so that it more closely approximates the ideal thin lens, but the fabrication will become more expensive and difficult and performance will be degraded by the inevitable flaws and dead space at the step boundaries that has been observed with material Fresnel lenses[22] and by the bowing and gradients of the fields across the gap that we have reported here. Since the focusing of the CMRL is wavelength dependent, a shorter center wavelength would require more elements and produce lower gains while longer center wavelengths would require fewer elements and more closely approximate the thin-lens case. Further improvement can be accomplished by using a tapered lens profile in which the height of the lens elements is decreased and either their thickness decreased or curvature increased as the elements near the sample side of

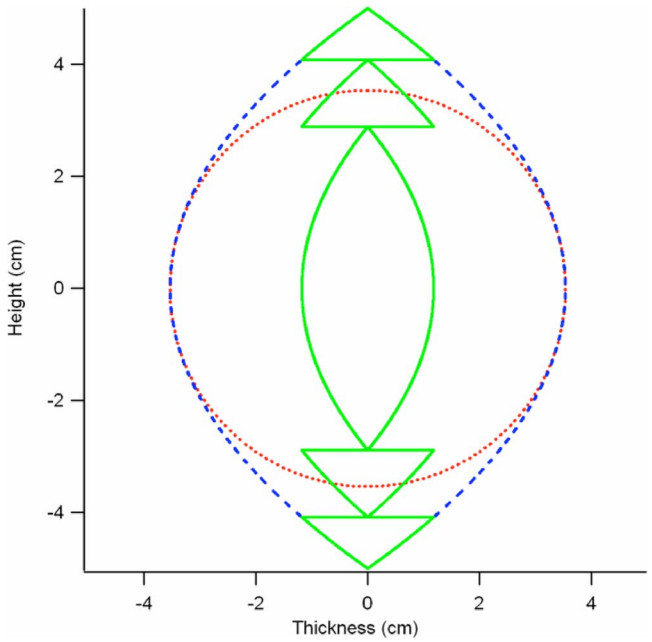

FIG. 10. (Color online) A comparison of different lens profiles: the circular lens such as demonstrated experimentally in this article (red, dotted), the parabolic lens with the same focal length as this circular lens in the paraxial limit (blue, dashed), and the same parabolic lens as a three-step Fresnel lens (green, solid).

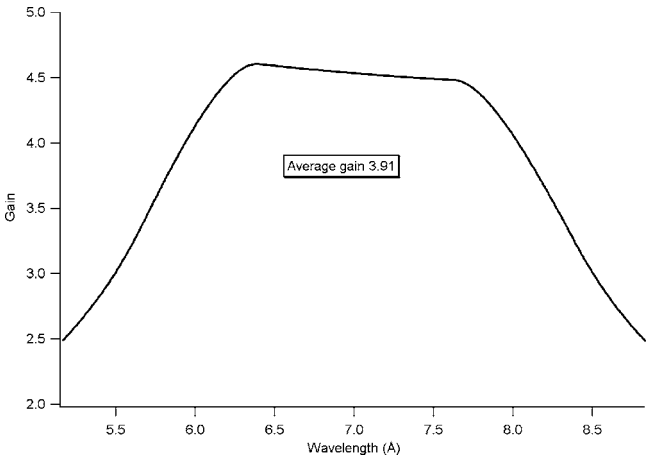

FIG. 11. Intensity gain as a function of wavelength calculated for the instrument and CMRL geometry sketched in Fig. 9.

the lens. This example shows that it is possible to use a CMRL lens to boost the performance of a practical slit-geometry instrument.

So far, only the shape of the magnets that create the field regions has been discussed, while it is assumed that beyond the poles the field rapidly drops to zero. It is noteworthy to point out that it is the change and the sharpness of the change in the magnetic field that determines the effective refractive index. This means, transitions between fields of opposite direction could double the focusing power, without increasing the magnitude of the field. Advanced engineering of the magnetic circuit would be required to make this feasible.

As discussed above, the performance of the tested lens described here was limited by both its geometry and the design of the magnetic circuit. Despite this, our results clearly demonstrate that compound magnetic refractive lenses offer a cost-effective way to boost intensity and improve the purity of the polarization of long-wavelength neutron beams. Furthermore, they do so without introducing additional material into the flight path which would attenuate or scattering the beam. We have discussed possible methods of boosting performance by using pole pieces with parabolic or Fresnel-lens sectional geometry. Finally, we have shown that a CMRL device with reasonable design parameters is a practical way to boost the intensity on small samples in slit-geometry instruments such as reflectometers located on pulsed, cold neutron sources like the SNS.

By using one-dimensional focusing, it is possible to decouple the focusing conditions in the orthogonal directions and thus perform independent optimizations for instruments with asymmetric requirements. This successful demonstration of one-dimensional focusing invites consideration of whether or slit-geometry instruments such as reflectometers or spin-echo instruments can be designed to simultaneous benefit in terms of both intensity and resolution enhancement through the use of focusing as had been shown to be true for small angle scattering instruments.

ACKNOWLEDGMENTS

The authors would like to thank R. Kleb and R. Vitt of the Intense Pulsed Neutron Source (ANL) for their technical assistance during the initial developments of the project, and Dihong Yu (ANSTO) for support during the experiment on ASTERIX. Work at Argonne was supported by the Department of Energy, Office of Sciences, under Contract No. DE-AC02-06CH11357. This work has benefited from the use of the Lujan Neutron Scattering Center at LANSCE, which is funded the Department of Energy's Office of Basic Energy Sciences. Los Alamos National Laboratory is operated by Los Alamos National Security LLC under DOE Contract No. DE-AC52-06NA25396.

APPENDIX

We recall here the basic optical expressions[10] that give the focusing properties of a compound refractive lens of thickness t. The coordinate z is along the optical path of the central ray of a one-dimensional beam of total height $2x_0$. For a lens segment of length dz the focal length is $f_N t/dz$. Over that length there is a change in the direction of the ray passing through the lens which is given by the ratio of the ray height x to the focal length of the segment. The matrix formulation[10] relating height x and inclination α from the front surface to the back surface of the lens is given by

$$\begin{pmatrix} x_f \\ \alpha_f \end{pmatrix} = \mathbf{M} \begin{pmatrix} x_i \\ \alpha_i \end{pmatrix} = \begin{pmatrix} \cos(t/f_N)^{1/2} & (f_N t)^{1/2} \sin(t/f_N)^{1/2} \\ -\dfrac{1}{(f_N t)^{1/2}} \sin(t/f_N)^{1/2} & \cos(t/f_N)^{1/2} \end{pmatrix} \times \begin{pmatrix} x_i \\ \alpha_i \end{pmatrix}, \tag{A1}$$

in terms of the focus for the thin lens, as given by Eq. (5). We derive a relation for the focusing properties of a thick lens in terms of ρ_i, ρ_f, which are, respectively, the actual distance of the object from the front end of the lens and the distance of the image from the back end of the lens.

We define as "principal planes" those planes for which the object distance r_i, image distance r_f, and focal length f are combined to give the thin lens result,

$$\frac{1}{f} = \frac{1}{r_i} + \frac{1}{r_f}. \tag{A2}$$

In terms of the actual distances ρ_i, ρ_f from the front and back end of the lens the focus is

$$\frac{1}{f} = \frac{1}{\rho_i + d} + \frac{1}{\rho_f + d}. \tag{A3}$$

The quantities d and f can be determined in terms of the matrix $\mathbf{M}$ given by Eq. (A1),

$$\mathbf{M} = \begin{pmatrix} 1 & d \\ 0 & 1 \end{pmatrix} \begin{pmatrix} 1 & 0 \\ -1/f & 1 \end{pmatrix} \begin{pmatrix} 1 & d \\ 0 & 1 \end{pmatrix}. \tag{A4}$$

The solution of Eq. (A4) is

$$\frac{f}{f_N} = \frac{\sqrt{t/f_N}}{\sin(\sqrt{t/f_N})}, \tag{A5}$$

$$d = f[1 - \cos(\sqrt{t/f_N})]. \tag{A6}$$

Once the effective focus and d are defined, the image distance ρ_f can be calculated for any object distance ρ_i.

For a sextupole lens the magnetic induction is given by

$$\mathbf{B} = \left(\frac{B_{\max}}{r_a^2}\right)(y^2 - x^2\ 2xy\ 0), \tag{A7}$$

and thus is radially constant[24] but increases quadratically from the center ($B=0$) to the boundary radius ($B=B_{\max}$). Since the equation of motion of the neutron in a magnetic field in the adiabatic limit is

$$\frac{d^2x}{dt^2} = \mp (|\mu|/m)\,\nabla\,|\mathbf{B}|, \tag{A8}$$

the optical transfer formula for the sextupole lens is

$$\begin{pmatrix} x_f & y_f \\ \alpha_f & \beta_f \end{pmatrix} = \begin{pmatrix} \cos(\omega L/v) & (v/\omega)\sin(\omega L/v) \\ -(\omega/v)\sin(\omega L/v) & \cos(\omega L/v) \end{pmatrix} \times \begin{pmatrix} x_i & y_i \\ \alpha_i & \beta_i \end{pmatrix}, \tag{A9}$$

for neutrons with spin parallel to the sextupole field.[24] Here α and β are the direction cosines relative to the x and y axes, respectively, L is the length of the lens, $v=h/m\lambda$ is the neutron velocity, and $\omega^2=2B_{\max}|\mu|/r_a^2 m$. The matrix in Eq. (A9) is formally identical to Eq. (A1), using the expression for the sextupol's focal length given in Eq. (6).

[1] K. Halbach, Nucl. Instrum. Methods **169**, 1 (1980).
[2] H. M. Shimizu *et al.*, Nucl. Instrum. Methods Phys. Res. A **430**, 423 (1999).
[3] J. Suzuki, T. Oku, T. Adachi, H. M. Shimizu, T. Hirumachi, T. Tsuchihashi, and I. Watanabe, J. Appl. Crystallogr. **36**, 795 (2003).
[4] A. Snigirev, V. Kohn, I. Snigireva, and B. Lengeler, Nature (London) **384**, 49 (1996).
[5] B. Lengeler, C. G. Schroer, M. Richwin, J. Tümmler, M. Drakopoulos, A. Snigirev, and I. Snigireva, Appl. Phys. Lett. **74**, 3924 (1999).
[6] D. A. Arms, E. M. Dufresne, R. Clarke, S. B. Dierker, N. R. Pereira, and D. Foster, Rev. Sci. Instrum. **73**, 1492 (2002).
[7] S. Bohic, A. Simionovici, A. Snigirev, R. Ortega, G. Devès, D. Heymann, and C. G. Schroer, Appl. Phys. Lett. **78**, 3544 (2001).
[8] M. R. Eskildsen, P. L. Gammel, E. D. Isaacs, C. Detlefs, K. Mortensen, and D. J. Bishop, Nature (London) **391**, 563 (1998).
[9] S. M. Choi, J. G. Barker, C. J. Glinka, Y. T. Cheng, and P. L. Gammel, J. Appl. Crystallogr. **33**, 793 (2000).
[10] K. D. Möller, *Optics* (University Science Books, Mill Valley, CA, 1988).
[11] W. Just, C. S. Schneider, R. Ciszewski, and C. G. Shull, Phys. Rev. B **7**, 4142 (1973).
[12] NdFeB 45, remanence MMC corporation, Hauppage, NY.
[13] M. R. Fitzsimmons and C. F. Majkrzak, in Modern Techniques for Characterizing Magnetic Materials, edited by Y. Zhu (Kluwer, Boston, 2005).
[14] T. Keller, T. Krist, A. Danzig, U. Keiderling, F. Mezei, and A. Wiedenmann, Nucl. Instrum. Methods Phys. Res. A **451**, 474 (2000).
[15] J. Major, H. Dosch, G. P. Felcher, K. Habicht, T. Keller, S. G. E. te Velthuis, A. Vorobiev, and M. Wahl, Physica B **336**, 8 (2003).
[16] M. Th. Rekveldt, Nucl. Instrum. Methods Phys. Res. B **114**, 366 (1996).
[17] R. H. Pantell, J. Feinstein, H. R. Beguiristain, M. A. Piestrup, C. K. Gary, and J. T. Cremer, Appl. Opt. **42**, 719 (2003).
[18] V. G. Kohn, J. Exp. Theor. Phys. **97**, 204 (2003).
[19] Z. Le and J. Liang, J. Opt. A, Pure Appl. Opt. **5**, 374 (2003).
[20] T. E. Mason, Phys. Today **59**(5), 44 (2006).
[21] T. Oku *et al.*, Nucl. Instrum. Methods Phys. Res. A **462**, 435 (2001).
[22] T. Adachi, J. Appl. Crystallogr. **36**, 806 (2003).
[23] C. G. Schroer and B. Lengeler, Phys. Rev. Lett. **94**, 054802 (2005).

[24] In the sextupole the magnetic fields are directed radially. To maintain the polarization of all neutrons along a definite direction, the neutrons are polarized in the direction of the beam before the lens, where the polarization is rotated adiabatically toward the radial direction. At the exit of the lens the reciprocal process takes place.